TiO_2 Based Thick Film pH Sensor

Mitar Simić, *Student Member, IEEE*, Libu Manjakkal, Krzystof Zaraska, Goran M. Stojanović, *Member, IEEE,* and Ravinder Dahiya, Senior *Member, IEEE*

***Abstract*— Miniaturized electrochemical pH sensors are increasingly in demand for application such as online monitoring of water quality and health monitoring. The metal oxides are the best candidates for sensing electrodes of such sensors as they offer high chemical stability. In this work, we present a novel approach to obtain interdigitated conductimetric pH sensor using screen printing of TiO_2 thick film on an alumina substrate. The microstructural and crystalline properties of the TiO_2 sensitive film were examined with scanning electron microscopy and Raman spectroscopy. The impedance spectroscopic studies of the fabricated thick film sensor were carried out in the frequency range of 5-20 kHz for the test solutions in the pH range of 4-10 and it was observed that the impedance of the film distinctly dependent on pH. Using the measured impedance data, we have also proposed an equivalent RC network model for the fabricated pH sensor. The physical meaning of the model parameters was determined by electrochemical impedance spectroscopic (EIS) analysis, and through statistical analysis it was found that all parameters are distinctly pH-dependent.**

***Index Terms*— pH Sensor, TiO_2 thick film, Conductimetric sensors, Electrochemical Impedance Spectroscopy, Electrical Equivalent circuits.**

I. Introduction

THE monitoring of water quality is an essential task having global impact. This requires determining the parameters such as pH, dissolved oxygen, content of ammonia, conductivity, turbidity, temperature, and dissolved metal ions, etc. [1]. Among these the pH is one of the most important as it measures the acidity or basicity of water and directly affects the health of individuals [2]. The pH measurement has wide range of application including environmental monitoring, chemical processing [3], medical [4], food and beverage [5], biomedical applications such as blood analysis [6], and monitoring of pH fluctuations in the human brain [7], etc. These applications require highly reliable and accurate pH sensors with the reduced level of maintenance and long lifetime. A range of electrochemical and non-electrochemical methods have been explored for pH measurement [8-10]. Among these the glass electrode based pH sensor have been most attractive and reliable [8-11]. However, the lack of applicability of existing solution in environments that are corrosion prone, or have high temperature and high pressure conditions is a limitation, which provides a strong motivation to develop new pH sensors. In this regards, the metal oxide based pH sensors are attractive as they offer a number of potential advantages over glass electrode pH sensors, including low-cost, smaller dimensions and ease of fabrication.

A few metal oxides based pH sensors and their deposition techniques have been reported in literature [9, 10]. The major works that have been carried out so far include metal oxides such as RuO_2, IrO_2, SnO_2, etc. as pH sensitive electrode. The poor cost-effectiveness of RuO_2 and IrO_2 based sensors [12, 13], low resistance of RuO_2 in alkaline solutions (which affect their lifetime) [12, 13], and buffer on the conductance in SnO_2 based conductimetric pH sensor [14]. etc. are some of the disadvantages of sensors based on above metal oxides. Further, many metal oxides based sensors working on potentiometric principle require a compatible reference electrode for miniaturization of the device [8, 15]. This is no needed in case of based pH sensors. Due to high chemical stability, the TiO_2 based films are considered good for pH sensitive layers and a few studies concerning TiO_2 as a pH sensing layer have been reported as well [16-17]. The major studies concerning TiO_2 based pH sensors include their use in ion sensitive field effect transistor (ISFET) and extended gate field effect transistor (EGFET) [18, 19]. However, in such realizations the sensors exhibited low sensitivity due to the intrinsic properties of TiO_2 films. Another disadvantage was that the reported sensors also required a reference electrode to operate. For these reasons, the pH sensors using metallic ion (Ru) doped TiO_2 or surface modification of the material by using TiO_2 nanotubes (NTs) or nanowires (NWs) were also proposed [17, 19]. The nanostructured surface array significantly increases the electrode surface area, which increases the number of adsorption sites for H_3O^+ ions and hence increases the pH sensitivity [17]. One example is the conductimetric pH sensor developed by Chen et al. [17], which is based on TiO_2/multiwall carbon nanotube (MWCNT)/cellulose hybrid nanocomposite. The fabricated sensor exhibited sensitivity in the pH range of 1-12. A large surface area of cellulose hybrid nanocomposite helps improve the pH sensitivity [17].

This work was partially supported by European Commission through grant numbers PITN-GA-2012-289481-SENSEIVER, PITN-GA-2012-317488-CONTEST, and EPSRC Engineering Fellowship for Growth – PRINTSKIN (EP/M002527/1). The authors are grateful to the Elvira Đurđić, University of Novi Sad, Serbia for Raman experiment and Dr. Carlos Garcia Nuñez and Dr. Dhayalan Shakthivel, BEST Group, University of Glasgow for useful feedback about the paper. We are also thankful to Electronic Systems Design Centre for the support related to characterization of sensors.

Mitar Simić is with Faculty of Electrical Engineering, University of Banja Luka, Republic of Srpska, Bosnia and Herzegovina.

Libu Manjakkal and Krzysztof Zaraska is with the Institute of Electron Technology, Krakow, Poland

Goran Stojanović is with Faculty of Technical Sciences, University of Novi Sad, Serbia

Libu Manjakkal and Ravinder Dahiya is with University of Glasgow, U.K (e-mail: Ravinder.Dahiya@glasgow.ac.uk.)

Advancing the state of the art, in this work we report our approach towards realizing portable, low-cost microcontroller-based pH monitoring system. We have designed, fabricated and characterized the interdigitated electrodes (IDE) based pH sensor on TiO_2 thick film. We have also designed and an impedance measurement system based on the integrated circuit AD5933 [20-22] which can be used for sensor impedance characterization as well as sensor readout electronics as a part of pH measurement system. The measured complex impedance data were theoretically analyzed with an electrical equivalent circuit model of the sensor.

This paper is organized as follows: Section II describes the fabrication steps of the sensor and the measurement system. In Section III, the structural properties of the film, the EIS analysis of the sensor with equivalent circuit model and the transfer function of the sensor in polynomial form are presented. Finally, the main results are summarized and directions of future work are discussed in the concluding Section IV.

II. Experimental

A. Sensor fabrication

The TiO_2 based conductimetric IDE pH sensor was fabricated using thick film technology. The fabrication procedure of the conductimetric pH was similar to that reported in [2, 23]. We chose alumina as a substrate to investigate the performance of pure metal oxide and to avoid any reaction at metal-metal oxide interface. Initially, a planar IDE was deposited on an alumina substrate by screen printing of Ag paste (Ag/Pd ESL 9695). Screen printing of metal paste is interesting as it is faster way of fabricating devices at low cost and is close to the manufacturing [24]. The electrode pattern consists of 0.5 mm wide and 10 mm long fingers with 0.5 mm distance between the adjacent fingers. The conducting layer was dried at 120°C for 20 min, and then the IDE structure was annealed at 850°C for 30 min. Subsequently, the TiO_2 sensitive layer was printed on the top of the IDE using screen printing. Dimensions of the sensitive rectangular layer are 17 x 13 mm^2. The TiO_2 paste for the sensitive film was prepared by mixing TiO_2 powder (99.8%, Aldrich) in ethyl cellulose binder and terpineol solvent in an agate mortar for 1 h. The sensitive layer was dried at 120°C for 20 min for solvent evaporation. The schematic image of the fabricated conductimetric pH sensor is shown in Fig. 1a.

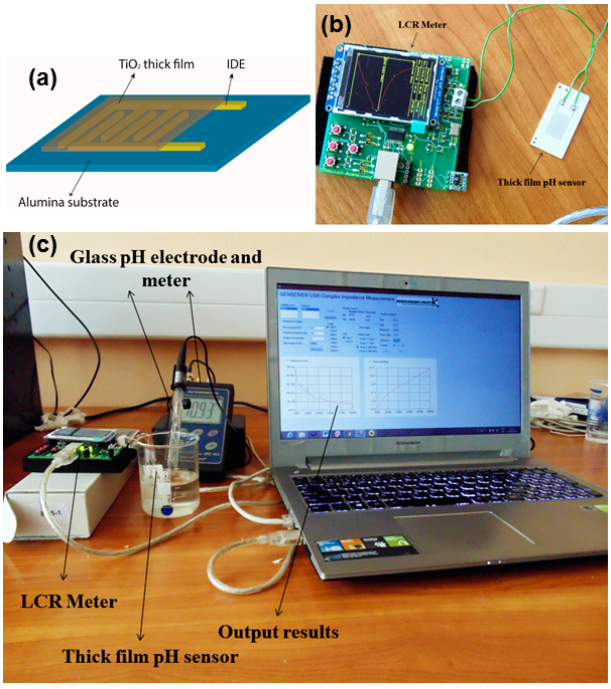

Fig. 1. (a) Schematic image of fabricated TiO_2 pH sensor, (b) Impedance measurement device connected with thick film pH sensor and (c) Experimental set-up for pH sensor characterization.

The major advantages of the fabricated IDE pH sensor, compared to other reported approaches in the literature are: faster and low-cost of fabrication, lack of reference electrode, large surface area and low power consumption during measurement. In addition, the screen printing technology cold open avenues for realizing the pH sensors in conjunction with electronics on flexible substrates [24].

B. Impedance measurement system

The AD5933-based impedance measurement system reported earlier [20-22] was used in this work for sensor characterization. The developed system can be battery powered, should a portable and autonomous operation is needed for *in-situ* measurements. The main features of this system are maximum relative error of 2 %, low cost, small dimensions, and optional full standalone operability. Amplitude of the output AC voltage can be selected as one from four options: 200, 400, 1000 and 2000 mV. The output signal is DC-free to prevent electrode polarization effect, which is very important in impedance spectroscopy. The system includes a thin film transistor (TFT) display, an embedded keypad, an SD card for data storage, as well as Personal Computer (PC) software (Fig.1b and 1c). Moreover, the device has self-calibration system and implemented algorithm for auto-ranging in impedance measurement. Thus, no additional components are required or manual range switching during the measurement which ensures rapid and automated operation. Analog front electronics for signal conditioning was developed in such a way that the presented system operates in two-electrode mode.

C. Measurements

The surface morphology and cross-sectional microstructure of TiO_2 films on alumina substrate were inspected by using scanning electron microscopy (SEM) (FEI Nova Nano, SEM 200, USA). The crystal structure of the prepared TiO_2 film was confirmed by using Raman spectroscopy. The Thermo Fisher DXR Raman microscope (USA) which had a diode-pumped solid-state (DPSS) laser with a wavelength of 532 nm, power level of 9 mW and the exposure time of 30 s was used for the film characterization.

Fig. 1c shows the experimental set-up for impedance

spectroscopic analysis of the sensor. The sample under test was connected to the measurement device and placed into a beaker with a solution. The fabricated sensor is proposed for water pollution monitoring, with expected operating pH range from 6 to 9, thus test solutions with pH ranging from 4 to 10 were prepared by adding 1 mol% of HCl or KOH to distilled water. A standard glass electrode pH and conductivity meter (ELMEIRON, CPC-411) with temperature probe, was applied to control the pH level of test solutions and to confirm the conductivity value of each pH test solution. The sensor was washed with deionized water and dried with paper towel after each measurement to reduce the contamination of electrode surface by the solution of another pH. The impedance measurement device was connected with PC, so developed C# application was used for acquisition of measurement data. All measurements were done at room temperature with liquid temperature close to the 23°C. To measure the electrical parameters of the TiO_2 films at different pH values, the sensor was dipped in solution for 10 min prior to operating to ensure stabilization. The impedance measurement was done by performing frequency sweep in range of 5-20 kHz with an AC voltage of 200 mV. The lowest amplitude of test signal was chosen to avoid excessive perturbation of the sample. With laboratory impedance measurement devices, usually it is possible to obtain impedance data in very wide frequency range, starting from few mHz to range of MHz. Such experimental data can provide more information about sensor behavior, but the limitations of developed impedance measurement device did not allow us to measure a wide frequency range. However, this is not an issue for this work as the main purpose here was to examine properties of fabricated sensor in frequency range in which reliable *in-situ* measurements can be performed with developed AD5933-based readout electronics. The obtained complex impedance data was analyzed with equivalent circuit developed with Multiple EIS Parameterization (MEISP) software [25].

III. Results and Discussion

A. Structural analysis

Fig. 2 shows the microstructure of TiO_2 thick film on an alumina substrate. The cross-sectional SEM image of the film is presented in Fig. 2a. The compatibility of this layer with the alumina substrate is very good. From Fig 2, it may be noted that the thickness of the screen printed film is nearly 7 µm. The TiO_2 thick film obtained in this work is homogeneous, with smooth surface, nanometric pores and grain sizes ranging from 180 to 225 nm (Fig. 2b).

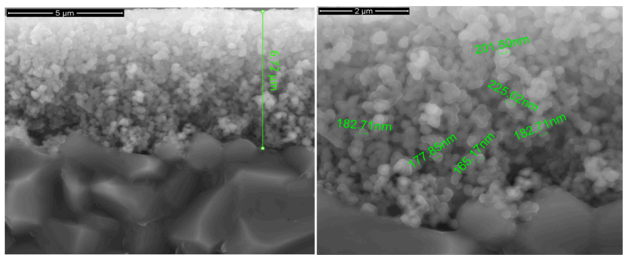

(a) (b)

Fig. 2. SEM images of TiO_2 thick film (a) cross-sectional view and (b) film microstructure with indication of grain sizes.

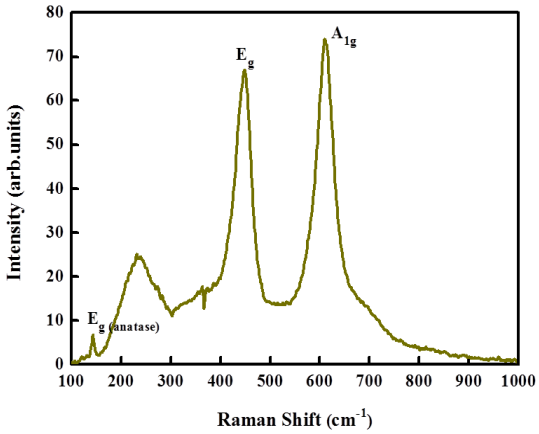

Fig. 3. Raman spectra of TiO_2 based thick films on alumina substrates.

Fig. 3 shows the Raman spectrum of TiO_2 thick film intered at 800°C on an alumina substrate. The higher annealing temperature is used this work as at these temperatures the the concentration of defects (O^- and Ti vacancies) in the TiO_2 films is reduced. Further, high temperature annealing results in large rutile grains [26]. In general, TiO_2 belongs to a rutile, anatase and brookite crystal structure [27]. The Raman spectra obtained for the thick film shows rutile and anatase spectral features of TiO_2 [28]. TiO_2 rutile structure belongs to the tetragonal crystal system. The peak observed at 143 cm^{-1} represents E_g anatase mode. However, for a rutile structure the doubly degenerate mode E_g was observed at a peak position of 448 cm^{-1}. In this peak position at 448 cm^{-1} and 610 cm^{-1} are very intense. Peak position at 610 cm^{-1} represents the symmetric mode A_{1g}. A broad peak is observed at 232 cm^{-1} and it may be due to infra-red active doubly degenerate mode of species E_u [28]. It is reported in literature that the E_g peak related to anatase phase of TiO_2 at 450°C and its intensity are high as compared to other peaks [28]. However, in our study the relative intensity of both E_g peaks and other peaks increases as a result of higher annealing temperature (800°C). This closely matches with similar observations in the literature [29, 30]. The presence of the anatase phase and absence of the rutile phase for films annealed up to 700°C is known from previous studies [30]. But for the films annealed at 800-1000°C the diffraction pattern shows peaks of both anatase and rutile reflections [30]. The increase in the intensities of all peaks in Raman patterns with annealing temperature also confirming improvement in the crystallinity of the films [30].

B. Impedance spectroscopic analysis of the sensor

The sensing performance of the TiO_2 based conductimetric pH sensor was tested by immersing the sensor in a solution with known pH. In an impedancemetric and/or conductimetric based sensor, any changes that occur on the surface of the sensitive electrode while reacting with solution, changes the electrical properties of the sensor [2, 14, 23, 31].

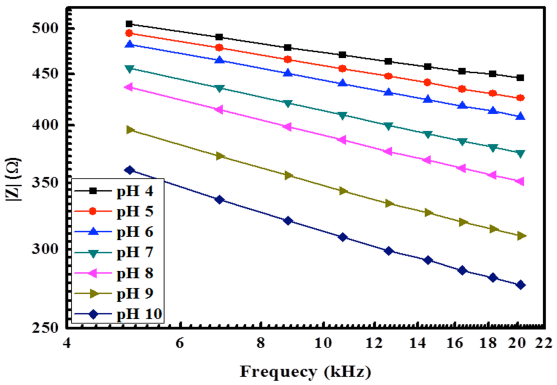

Fig. 4. Bode impedance plot for TiO_2 thick film pH sensor for different pH values of solutions over the frequency range of 5-20 kHz.

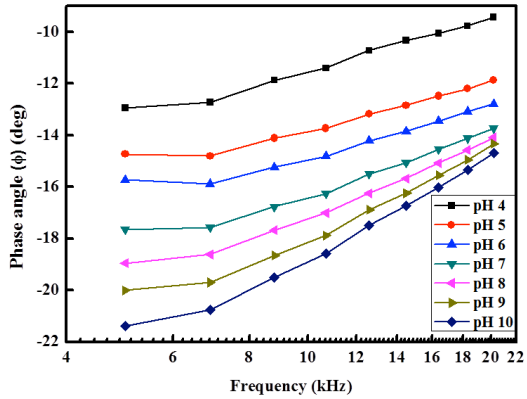

Fig. 5. Bode phase magnitude plot for TiO_2 thick film pH sensor for different pH values of solutions over the frequency range of 5-20 kHz.

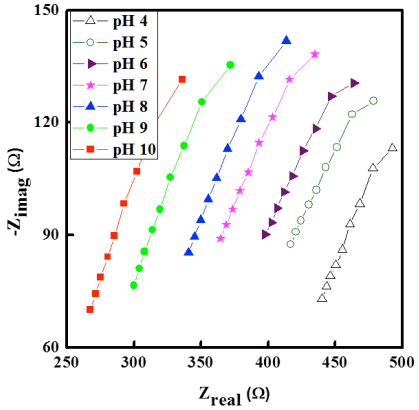

Fig. 6. Nyquist plot for TiO_2 thick film pH sensor for different pH values of solutions over the frequency range of 5 - 20 kHz.

Fig. 4 and 5 illustrate the variation of impedance magnitude and phase angle as a function of frequency in the range 5-20 kHz for different pH values of test solution. The impedance as well as phase of our sensors decrease with increase in the pH value of solution. For a constant pH, we see decrease in the impedance and increase in phase as the frequency increases. These changes in impedance and phase of TiO_2 based sensor can be attributed to electrochemical surface reaction of H^+/OH^- ions with the oxide surface. When a metal oxide is introduced into an electrolyte, many electrochemical reactions occur at the oxide-solution surface [2, 23]. In the case of TiO_2, the dissociative chemisorption of water molecule results in the formation of surface hydroxyl group [15]. Due to adsorption/diffusion of H^+/OH^- ions the surface of TiO_2 becomes charged and it creates an electrical double layer structure by site binding theory [23, 32]. With changes in the pH of a solution the contribution of both H^+ and OH^- ions also varies. In an IDE based structure, the applied potential and the conductivity of solution have strong influence on the electrical parameters and sensitivity.

From Fig. 4, it can be noted that the impedance is lower when the sensor is in a solution of a higher pH. Variations in the solution resistance with different pH values contribute to the changes in impedance of the sensor. The observed dependence is mainly caused by a lower resistance of applied alkaline solutions as compared with the acidic solutions. The variation in impedance with frequency can be attributed to the effect of intercrystalline capacitance [14]. In the kHz-range, this value is sufficient for short-circuiting the spaces between the grains, and hence can reduce the resistance of sensor [14].

More detailed information regarding the complex impedance of the sensor can be observed by using a Nyquist plot. The Nyquist plot displays imaginary part (Z_{imag}) versus real part (Z_{real}) of impedance as a function of the frequency [33]. The Nyquist plot for the analyzed TiO_2 based pH sensor is shown in Fig. 6. Observed behavior of the sensor from the Nyquist plot in analyzed frequency range, was discussed in more details in Section III.C, but a large incomplete arc in the Nyquist plot is possibly due to charge transfer and ion exchange at the surface of the material while reacting with ions in the solution [14, 23, 31].

The variation of the electrical parameters and pH sensitivity also depends on the microstructural properties of the material such as porosity, thickness, composition, crystalline structure and homogeneity of the surface [2, 23, 31]. In particular, the porosity of sensing electrode plays a significant role in defining the sensing performance. The SEM analysis of TiO_2 thick film (Fig. 2) shows that it is porous, which means the ions from the solution can easily penetrate into the layer and react with metal oxide molecules at the grain boundaries. If an intermediate step of electrochemical reaction exhibits strong adsorption/diffusion to the electrode surface, a high-frequency impedance of electrochemical double layer can be expressed by electrical equivalent circuit presented in Fig. 7, as proposed in [34, 35].

A similar equivalent circuit model was described in our previous RuO_2 based thick film pH sensor [23]. The physical meaning of the parameters of the proposed equivalent electrical circuit are as follows: R_s represents solution

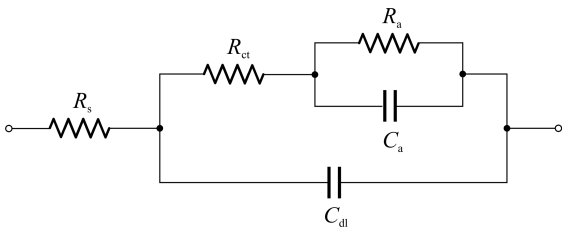

Fig. 7. Schematic presentation of the proposed equivalent RC network.

resistance, R_{ct}, is charge transfer resistance, C_{dl} is double layer capacitance, R_a is resistance associated with activation energy of the adsorption/desorption and C_a is associated with maximal amount of adsorbed specie.

Impedance of this RC network (Fig. 7), at some angular frequency ω [rad/s], is defined as:

$$Z(\omega) = R_s + \frac{1}{\frac{1}{R_{ct} + \frac{1}{\frac{1}{R_a} + j\omega C_a}} + j\omega C_{dl}} \quad (1)$$

In the present study, various parameters of equivalent circuit such as R_s, R_{ct}, C_{dl}, R_a and C_a, are estimated with data fitting in MEISP software and are presented in Table I.

TABLE I
ESTIMATED VALUES FOR MODEL PARAMETERS FOR DIFFERENT PH VALUES

pH Value	R_s [Ω]	R_{ct} [Ω]	C_{dl} [F]	R_a Ω]	C_a [F]
4	396.37	169.39	$7.84\cdot10^{-8}$	$1.67\cdot10^{5}$	$2.75\cdot10^{-7}$
5	358.64	194.76	$6.15\cdot10^{-8}$	$1.26\cdot10^{5}$	$2.60\cdot10^{-7}$
6	340.51	204.28	$6.14\cdot10^{-8}$	$1.35\cdot10^{5}$	$2.52\cdot10^{-7}$
7	315.07	215.02	$6.71\cdot10^{-8}$	$1.22\cdot10^{5}$	$2.37\cdot10^{-7}$
8	299.08	222.01	$7.41\cdot10^{-8}$	$8.33\cdot10^{4}$	$2.31\cdot10^{-7}$
9	268.04	220.83	$8.77\cdot10^{-8}$	$1.50\cdot10^{5}$	$2.49\cdot10^{-7}$
10	241.18	214.56	$9.85\cdot10^{-8}$	$5.22\cdot10^{3}$	$2.54\cdot10^{-7}$

Estimated values for model parameters were used for impedance calculation using Equation (1) in the frequency range of 5-20 kHz. After that, the viability of the proposed model was evaluated by means of Root Mean Square Error (RMSE) calculation for calculated real and imaginary parts of impedance, compared to the measured values. In Table II, obtained RMSE values for all pH values are presented. From the obtained results, it can be noticed that all fittings results in RMSE value lower than 5 Ω. Moreover, it can be seen that RMSE values slightly decrease with increase of pH value.

TABLE II
RMSE VALUES FOR FITTING OF REAL AND IMAGINARY PART OF IMPEDANCE FOR DIFFERENT PH VALUES

pH Value	$RMSE_{real}$ [Ω]	$RMSE_{imag}$ [Ω]
4	3.964	3.111
5	4.566	3.873
6	4.658	3.996
7	4.401	3.310
8	3.977	2.570
9	3.379	2.076
10	2.844	1.633

As mentioned above, in the equivalent circuit, R_s represents the solution resistance, which depends on the conductivity of the pH solution. When preparing the pH solution, it was observed that while varying the pH value from 4 to 10 the conductivity of solution increases as shown in Fig. 8. It was measured by commercial conductivity meter (ELMEIRON, CPC-411). A similar result is observed in the equivalent circuit analysis. The value of R_s decreases with increasing alkaline nature of the solution as shown in Table I.

The charge transfer resistance (R_{ct}) depends on surface properties of sensing material, pH value, and conductivity of the solution. In general, the R_{ct} is associated with the resistance to process of electron transfer from electrode to

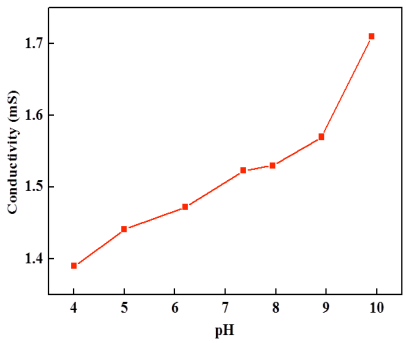

Fig. 8. Variation of solution conductivity with change in pH of solution

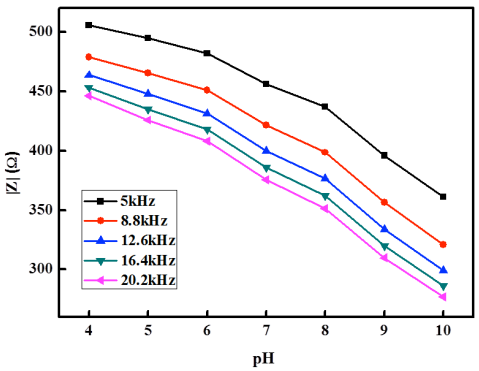

Fig. 9. Sample impedance versus pH at different frequencies.

electrolyte and vice versa. It can be seen from Table I, that the value of R_{ct} increases with the pH value.

Hence, in analyzed frequency range, R_{ct} and R_s play intensive role in sensor response. Compared to our previous study for a RuO_2 based sensor [23], the values of R_{ct} and R_s are higher in magnitude for TiO_2 based sensor. In addition to this, for RuO_2 based sensor, the highest pH values of R_{ct} was 6, however, for this TiO_2 based sensor, the highest pH value was observed to be 8. It may be due to different surface properties of the material.

In the equivalent circuit C_{dl} represents the double-layer capacitance and the generated capacitance C_a is due to adsorption or diffusion of ions at oxide-solution interface. The capacitance C_{dl} exists on the interface between an electrode and surrounding electrolyte. When a metal oxide is immersed in the solution, the double layer is formed because some ions from the solution diffuse onto the electrode surface. The value of C_{dl} may depend on variables such as electrode potential, temperature, ionic concentrations, types of ions, oxide layers, electrode roughness, and impurity adsorption, etc. [23]. The capacitance C_a depends on the activation energy due to ionic exchange from solution at the metal oxide surface. For IDE TiO_2 based pH sensor in the analyzed frequency range, the impedance parameters R_a (adsorption resistance) and C_a may be related to adsorption/diffusion of ions at the oxide surface-solution interface. Meanwhile, R_{ct} and C_{dl} are assigned to the charge transfer process. Hence, a mixed ionic and electronic conduction is responsible for observed behavior of TiO_2 based interdigitated pH sensor.

To get more information about the relationship between model parameters and pH value of the solution, a statistical

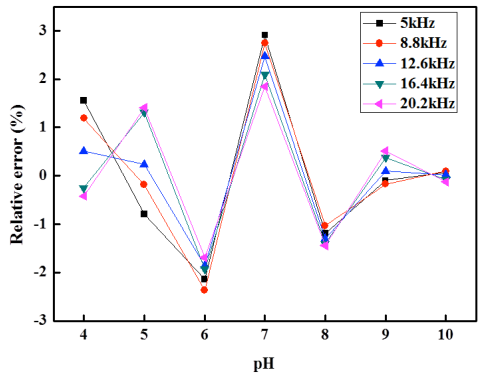

Fig. 10. Relative error in pH with 3rd order polynomial approximation of the sensor transfer function.

analysis was conducted. Two of the most common used statistical parameters are the Pearson correlation coefficient (r) and the coefficient of determination (r^2). The calculated values for Pearson correlation coefficients and coefficients of determination showed that the parameter that best correlates with pH is R_s (r=-0.996). A strong correlation can be found for R_{ct} as well (r=0.847), while for R_a, C_{dl} and C_a, correlation is weaker but still relatively strong (r=0.6-0.7). Thus, it can be noticed that the charge transfer and ion exchange are two dominant phenomena for the sensing performances of the IDE TiO_2 pH sensor. Moreover, it was found that all model parameters are distinctly pH-dependent.

We have also analyzed the effect of each parameter of equivalent circuit on the overall impedance of sensor. This was done by analyzing the proposed equivalent electric circuit (Fig. 7) and the model parameters presented in Table I. In the analyzed frequency range, impedance of parallel connection of R_a and C_a is dominantly defined by C_a due to fact that, even on low frequencies, impedance magnitude of C_a is much lower than R_a. This can be treated as C_a short-circuiting the R_a. This effect is larger at higher frequencies and it occurs for each pH value. Thus, the upper branch of equivalent electric circuit can be approximately considered as series of R_{ct} and C_a. By direct comparison of impedances at each pH value, it can be seen that R_{ct} has higher value even in the low frequency regime. Thus, the equivalent circuit (Fig. 7) can be simplified as a R_s in series with parallel connected R_{ct} and C_{dl}. From Table I, it can be seen that R_s decreases with increase in pH value while R_{ct} increases. However, the influence of R_{ct} is diminished at higher frequencies by C_{dl} and this effect is larger for higher pH values. This observation correlates very well with Fig. 5 from which can be seen that phase angle of equivalent circuit decreases with increase in the pH, thus clearly manifesting the capacitive behavior.

C. *Transfer function of the sensor in polynomial form*

Towards the implementation of portable and autonomous microcontroller-based system for remote pH monitoring, the transfer function of the sensor in polynomial form is needed. This approach ensures simple implementation where polynomial curve fitting coefficients can be stored in memory of microcontroller as look-up table.

To obtain a sensor's transfer function in such form, it is required to have a relationship between the magnitude, phase angle, real or imaginary part of impedance of the sample with pH value for fixed frequency. However, the use of impedance magnitude, $|Z|$, offers advantage over use of the impedance phase angle because phase detector is not required, which can significantly reduce a complexity of measurement device. Thus, the impedance magnitudes of the fabricated sample versus pH value for six different frequencies (5, 8.8, 12.6, 16.4 and 20.2 kHz) are plotted in Fig. 9. These values were chosen to ensure linear distribution in analyzed frequency range.

With this data, a polynomial curve fitting can be used to obtain the transfer function of the sensor, $pH(|Z|)$:

$$pH(|Z|) = p_1|Z|^n + p_2|Z|^{n-1} + \ldots + p_n|Z| + p_{n+1} \qquad (2)$$

where $|Z|$ is impedance magnitude of the sensor, n is order of polynomial and p_i (i=1..n+1) are polynomial curve fitting coefficients.

For pH range from 4 to 10 it is necessary to have 6th order polynomial. With this high order polynomial, the error is usually very small and theoretically it should be zero. The disadvantage of this approach is that a complex mathematical operation is required for pH computation. The order of the polynomial can be lower, but that will introduce error in pH measurement. The advantage of this approach is that the complexity of pH computation procedure is reduced and it is less time consuming. In Table III, a 3rd order polynomial curve fitting coefficients is for used test frequencies. Relative errors in pH estimation with 3rd order polynomial approximation of sensor transfer function are presented in Fig. 10.

TABLE III
3RD ORDER POLYNOMIAL CURVE FITTING COEFFICIENTS

***f* [kHz]**	p_1	p_2	p_3	p_4
5	$-2.10\cdot10^{-6}$	$2.54\cdot10^{-3}$	-1.05	156.48
8.8	$-1.50\cdot10^{-6}$	$1.66\cdot10^{-3}$	-0.64	92.83
12.6	$-1.06\cdot10^{-6}$	$1.10\cdot10^{-3}$	-0.41	61.64
16.4	$-8.24\cdot10^{-7}$	$8.17\cdot10^{-4}$	-0.30	47.24
20.2	$-6.14\cdot10^{-7}$	$5.84\cdot10^{-4}$	-0.21	36.99

Compared to modeling of sensor with equivalent electrical circuit the advantage of our approach where transfer function of sensor is presented in polynomial form, is the easy realization of portable and autonomous microcontroller-based system for remote pH monitoring. Moreover, pH value of unknown solution can be obtained. However, the disadvantage is that there is no information about physical processes occurring at the sensor-solution interface.

IV. Conclusion

In this work, a thick film interdigitated TiO_2 based conductimetric pH sensor has been presented. The impedance measurement system, developed with integrated circuit AD5933, was used for impedance characterization of the sensor in frequency range of 5-20 kHz. The device is designed to enable the portable and autonomous operation for *in-situ* measurements as well as laboratory characterization of the sample. The obtained results showed that both, impedance magnitude and phase angle, are frequency- and pH-dependent.

The SEM image showed the nanocrystaline structure (grain

size in the range of 160 to 230 nm) of the sensitive film. The crystalline structure of the TiO_2 film observed using Raman spectroscopy revealed the presence of both anatase and rutile structure. The impedance spectroscopy analysis shows that the electrical parameters of the sensor are strongly dependent on the pH of solution in the low frequency range. The obtained complex impedance data of the sensor were also analyzed with RC equivalent circuit and it was observed that charge transfer and ion exchange are the two dominant phenomena for the sensing performances of an interdigitated TiO_2 pH sensor.

As a future work we are working towards fabricating the pH sensor on a flexible substrate by using nanostructured powder of TiO_2. This will address the needs for chemical sensors in wearable devices for healthcare applications. A major challenge for TiO_2 based pH sensor on flexible substrates will be posed by the high-temperature processing requirements, especially for the thick film technology presented here. We aim to use transfer printing method to overcome such challenges. We have successfully used transfer printing method to overcome the similar thermal budget issue in case of silicon based flexible electronics [36-38]. In addition to this we will also miniaturize the LCR meter for potable online monitoring applications over a wide range of frequencies.

REFERENCES

[1] J. Kang, M. Wang and Z. Xiao, "Modeling and Control of pH in Pulp and Paper Wastewater Treatment Process," *J. Water Resource and Protection*. *2*, pp. 122-127, 2009.

[2] L. Manjakkal, K. Cvejin, J. Kulawik, K. Zaraska, D. Szwagierczak and R. P. Socha, "Fabrication of thick film sensitive RuO_2-TiO_2 and Ag/AgCl/KCl reference electrodes and their application for pH measurements," *Sensor. Actuat. B- Chem. 204*, pp. 57–67, 2014.

[3] H. A. Clark, R. Kopelman, R. Tjalkens and M. A. Philbert. (1999). Optical Nanosensors for Chemical Analysis inside Single Living Cells. 2. Sensors for pH and Calcium and the Intracellular Application of PEBBLE Sensors. *Anal. Chem. 71(21)*, pp. 4837-4843.

[4] B. D. Malhotra and A. Chaubey. (2003). Biosensors for clinical diagnostics industry. *Sensor. Actuat. B- Chem. 91*, pp. 117-127. Available: doi: 0.1016/S0925-4005(03)00075-3

[5] C. Bohnke, H. Duroy and J. L. Fourquet. (2003). pH sensors with lithium lanthanum titanate sensitive material: applications in food industry. *Sensor. Actuat. B- Chem. 89*, pp. 240-247.

[6] L. Xie, Y. Qin and H. Y. Chen. (2012). Polymeric Optodes Based on Upconverting Nanorods for Fluorescent Measurements of pH and Metal Ions in Blood Samples. *Anal. Chem. 84 (4)*, pp. 1969-1974.

[7] V. A. Magnotta, H. Y. Heo, B. J. Dlouhy, N. S. Dahdaleh, R. L. Follmer, D. R. Thedensa, M. J. Welshc and J. A. Wemmie. (2012). Detecting activity-evoked pH changes in human brain. *Proc. Natl. Acad. Sci. USA. 109* (*21*), pp. 8270–8273.

[8] U. Guth, W. Vonau, and J. Zosel. (2009). Recent developments in electrochemical sensor application and technology—a review. *Meas. Sci. Technol. 20*, pp. 1–14.

[9] Y. Qin, H. J. Kwon, M. M. Howlader and M. J. Deen. (2015). Microfabricated electrochemical pH and free chlorine sensors for water quality monitoring: recent advances and research challenges. *RSC Advances. 5(85)*, pp. 69086-69109.

[10] P. Kurzweil. (2009). Metal oxides and ion-exchanging surfaces as pH sensors in liquids: state-of-the-art and outlook. *Sensors*. *9*, pp. 4955–85.

[11] G. Eisenmann. (1967). *Glass electrodes for hydrogen and other cations*, Ed., Marcel Dekker, New York, NY, USA.

[12] E. Mayousse, F. Maillard, F. Fouda-Onana, O. Sicardy and. N. Guillet. (2011). Synthesis and characterization of electrocatalysts for the oxygen evolution in PEM water electrolysis. *Int. J. Hydrogen Energy*. *36*, pp. 10474-10481.

[13] G.M. da Silva, S.G. Lemos, L.A. Pocrifka, P.D. Marreto, A.V. Rosario, E.C. Pereira. (2010). Development of low-cost metal oxide pH electrodes based on the polymeric precursor method. *Anal. Chim. Acta*. 616, pp. 36–41

[14] K. Arshak, E. Gill, A. Arshak and O. Korostynska. (2007). Investigation of tin oxides as sensing layers in conductimetric interdigitated pH sensors. *Sensor. Actuat. B- Chem. 127*, pp. 42–53.

[15] A. Fog, R. P. Buck, (1984) Electronic semiconducting oxides as pH sensors, Sensor. Actuat. B-Chem., 5, pp. 137-146.

[16] Y. H. Liao and J. C. Chou. (2009). Preparation and characterization of the titanium dioxide thin films used for pH electrode and procaine drug sensor by sol-gel method. *Mat. Chem. Phys. 114*, pp. 542-548.

[17] Y. Chen, S. C. Mun and J. Kim. (2013). A wide range conductometric pH sensor made with titanium dioxide/multiwall carbon nanotube/cellulose hybrid nanocomposite. *IEEE Sensor. J. 13*, pp. 4157-4162.

[18] J. C. Chou and C.W. Chen. (2009). Fabrication and Application of Ruthenium-Doped Titanium Dioxide Films as Electrode Material for Ion-Sensitive Extended-Gate FETs. *IEEE Sensor. J. 9*, pp. 277-283.

[19] Y.C. Huang, F.S. Tsai and S.J. Wang. (2014). Preparation of TiO_2 nanowire arrays through hydrothermal growth method and their pH sensing characteristics. *Jpn. J. Appl. Phys. 53*, 06JG02, pp. 1-5.

[20] M. Simić. (2015). Complex impedance measurement system for the frequency range from 5 kHz to 100 kHz. *Key Engineering Materials*. *644*, pp. 133-136.

[21] M. Simić, "Realization of digital LCR meter", *in Proc. EPE*, 2014. pp. 769-773.

[22] M. Simić, "Complex impedance measurement system for environmental sensors characterization", in Proc. TELFOR, 2014. pp. 660-663.

[23] L. Manjakkal, E. Djurdjic, K. Cvejin, J. Kulawik, K. Zaraska and D. Szwagierczak. (2015). Electrochemical impedance spectroscopic analysis of RuO_2 based metal oxide thick film pH sensors. *Electrochim. Acta*. *168*, pp. 246-255.

[24] S. Khan, L. Lorenzelli and R. Dahiya. (2015). Technologies for Printing Sensors and Electronics Over Large Flexible Substrates: A Review. *IEEE Sensor. J. 15(6)*, pp. 3164-3185.

[25] MEISP, March 2002. Korea: Kumho Chemical Laboratories.

[26] C. S. Chua, X. Fang, X. Chen, O. K. Tan, M.S. Tse, A. M. Soutar X. and Ding. (2014). Effect of Annealing Temperature on Microstructure and UV Light Photocatalytic Activity of TiO_2 Films Grown by Atmospheric Pressure CVD. *Chem. Vap. Deposition. 20*, pp. 44–50.

[27] A. P. S. Krishnamurti. (1962). The Raman spectrum of rutile, *Proc. Indian Academy of Sciences, Section A*. *55*, pp. 290-299.

[28] T. Mazza, E. Barborini, P. Piseri, and P. Milani. (2007). Raman spectroscopy characterization of TiO_2 rutile nanocrystals. *Physical Review B*. *75*, pp. 045416(1-5).

[29] N. S. Gluck, H. Sankur, J. Heuer, J. DeNatale and W. J. Gunning. (1991). Microstructure and composition of composite SiO_2/TiO_2 thin films. *J. Appl. Phys*. 69, pp. 3037.

[30] H. Rath, S. Anand, M. Mohapatra, N. C. Mishra. (2009). Effect of thermal annealing on the structure and microstructure of TiO2 thin films. *Indian J. Phys*. *83(4)*, pp. 559-565.

[31] L. Manjakkal, K. Cvejin, B. Bajac B, J. Kulawik, K. Zaraska and D. Szwagierczak. (2015). Microstructural, impedance spectroscopic and potentiometric analysis of Ta_2O_5 electrochemical thick film pH sensors. *Electroanal*. *27*, pp. 770-781.

[32] D. E. Yates, S. Levine and T. W. Healy. (1974). Site-binding model of the electrical double layer at the oxide/ water interface. *J. Chem. Soc., Faraday Trans. 1*. 170, pp. 1807-1818.

[33] V. F. Lvovich. (2012). *Impedance spectroscopy application to electrochemical and dielectric phenomena*, John Willey & Sons. Inc. New Jersey.

[34] D. C. Grahame. (1952). Mathematical theory of the Faradaic admitance. *J. Electrochem. Soc*. *99*, pp. 370.

[35] H. Gerisher and W. Mehl. (1955). Zum Mechanismus der Kathodischen Wasserstoffabscheidung and Quecksilber, Silber, und Kupfer, *Z. Electrochem*., 59, pp. 1049.

[36] S. Khan, L. Lorenzelli, and R. Dahiya. (2016). Flexible MISFET Devices from Transfer Printed Si Microwires and Spray Coating. I*EEE J. Electron Device Society*, *4(4)*, pp. 189-196.

[37] R. Dahiya, G. Gottardi and N. Laidani. (2015). PDMS residues-free micro/macrostructures on Flexible Substrates. *Microelectron. Eng.*, 136, pp. 57-62.

[38] R. Dahiya, A. Adami, C. Collini and L. Lorenzelli. (2012). Fabrication of Single Crystal Silicon Mirco-/Nanostructures and Transferring them to Flexible Substrates. *Microelectron. Eng*., *98*, pp. 502-507.

Mitar Simić was born in 1987. He received the B.Sc. and M.Sc. degrees in electrical engineering from the University of East Sarajevo, Bosnia and Herzegovina, in 2010 and 2012, respectively. He is currently pursuing the Ph.D. degree in electrical engineering at University of Novi Sad. He is currently a Teaching Assistant at the University of Banja Luka. His research interests include impedance spectroscopy analysis, equivalent circuit modeling and development of devices for impedance measurement.

Libu Manjakkal received B.Sc. in Physics from Calicut University, India in 2006, M.Sc. in Physics from Mahatma Gandhi University, Kerala, India in 2008 and Ph.D. in electronics with honors from Institute of Electron Technology (ITE), Warsaw, Poland, in 2015. His Ph.D. thesis was related to metal oxide based thick film pH sensors.

In the period 2009–2012 he was involved in two research and development projects at C-MET, Thrissur, Kerala, India. He also worked in CEMOP/UNINOVA, New University of Lisbon, Portugal for the period May–July 2012. From 2012 to 2015 he worked as an Early Stage Researcher Fellow in the framework of Marie Curie ITN Program within the SENSEIVER project, at ITE, Poland. From 2015-2016 he worked as a postdoctoral researcher at ITE Poland. Currently he is working as a Marie Curie experienced researcher at BEST group, Electronics and Nanoscale Engineering Research Division, University of Glasgow, U.K. He is an author or co-author of 26 scientific papers. His current research interests comprise flexible and printable electronics, electrochemical sensors, LTCC technology, multilayer actuators, TCO films, pH sensors and gas sensors. He is a member of international microelectronics assembly and packaging society (IMAPS) Poland chapter.

Krzysztof Zaraska was born in Krakow, Republic of Poland, in 1980. He received M.Sc. degree in Telecommunication Networks and Systems from the AGH University of Science and Technology, Krakow, Poland, in 2004. He is the head of Laboratory of Microstructures in the Institute of Electron Technology, Krakow Division, Poland. He is an author or coauthor of 71 scientific papers. He managed the SENSEIVER FP7 project at ITE. His present research interests include wireless sensor application, LTCC technology, gas sensors, and pH sensors.

Professor Goran Stojanović was born in Smederevo, Republic of Serbia, in 1972. He received a B.Sc., M.Sc. and Ph.D. degrees, all in electrical engineering, from the University of Novi Sad in 1996, 2003 and 2005, respectively.

He is a full professor at the Faculty of Technical Sciences, University of Novi Sad, Novi Sad, Autonomous Province of Vojvodina, Republic of Serbia. He is an author or co-author of 155 scientific papers including 45 articles in leading international peer-reviewed journals (with impact factors). His research interest includes printed/organic/flexible electronics as well as nanoelectronics and application of advanced nano structured materials.

Prof. Stojanović is a reviewer of many leading international journals. Prof. Stojanović has almost ten years of experience in coordination and implementation of different EU funded projects.

Ravinder Dahiya (S'05, M'09, SM'12) is Reader and EPSRC (Engineering and Physical Sciences Research Council) Fellow in the School of Engineering at University of Glasgow, UK. He completed Ph.D. at Italian Institute of Technology, Genoa (Italy).

His multidisciplinary research interests include Flexible and Printable Electronics, Electronic Skin, Tactile Sensing, Robotics, and Wearable Electronics. He has published more than 150 research articles, 6 books (including 5 at various stages of publication) and 9 patents (including 7 submitted). He has worked on and has led many international projects funded by European Commission and EPSRC.

He is Distinguished Lecturer of IEEE Sensors Council (2016-2018) and senior member of IEEE. Currently he is serving on the Editorial Boards of IEEE Transactions on Robotics and IEEE Sensors Journal and has been guest editor of 4 Special Journal Issues. He is founding chair of the IEEE UKRI sensors council chapter. He was General Chair of IEEE PRIME 2015 and is the Technical Program Chair (TPC) of IEEE Sensors 2017.

He holds prestigious EPSRC Fellowship and received in past the Marie Curie Fellowship and Japanese Monbusho Fellowship. He was awarded with the University Gold Medal and received best paper awards 2 times and another 2 second best paper awards as co-author in international conferences.